Nuclear Science and Techniques **24** (2013) 050515

On ring and bubble formations in heavy ion collisions

CHEREVKO Kostyantyn[1,2,3] SU Jun[1,2] BULAVIN Leonid[3] SYSOEV Volodymyr[3]
ZHANG FengShou[1,2,4,*]

[1]*College of Nuclear Science and Technology, Beijing Normal University, Beijing 100875, China*

[2]*Beijing Radiation Center, Beijing 100875, China*

[3]*Physics Department, Taras Shevchenko National University of Kyiv, 4 Glushkova av., Kyiv 03022, Ukraine*

[4]*Center of Theoretical Nuclear Physics, National Laboratory of Heavy Ion Accelerator of Lanzhou, Lanzhou 730000, China*

Abstract The work is devoted to the implementation of the hydrodynamic laws to the head-on heavy ion collisions within the energy range 50–100 MeV/*A*. The hydrodynamic mechanisms of the bubble and ring structures formation are investigated. It is shown that there is a possible hydrodynamic explanation of the different structures being formed in the case of soft (*K*=200 MeV) and stiff (*K*=400 MeV) equations of state. Within the suggested approach the final geometry of the system is defined in the initial stage of the collision and is very dependent on the sound velocity in the nuclear matter. The obtained results are in a good correspondence with the Boltzmann-like transport theory calculations and the experimental data for the selected energy range.

Key words Nuclear incompressibility, Head-on collisions, Hydrodynamics.

1 Introduction

The knowledge of the nuclear equation of state (EOS) is one of the fundamental goals in nuclear physics[1-4] which has not yet been achieved[5,6]. The possibility of extracting information on the EOS at high baryon density, is restricted to two fields of research that are observations of astrophysical compact objects and studies of hot nuclear systems, created in high energy proton induced reactions or in heavy-ion collisions (HIC). Probably this explains the intensive studies of heavy ion collisions during the last several decades. The very exciting parts of them are the studies devoted to the nuclear multifragmentation (MF) when a number of intermediate mass fragments 3<*Z*<20 (IMF) are being formed from the compressed and excited system[7-9]. IMFs may provide a unique probe to study the reaction mechanism and hot nuclear matter properties[10]. In spite of such an interest to the topic, there are still many questions to be answered. The serious challenge in the studies is the inclusiveness of the heavy ion collisions experiments[11]. The nowadays detectors are very sophisticated and allow the high detection rate but still some data are missing[12]. At this step a powerful instrument of computer simulations is of high importance. There is a number of transport theories used for simulating collisions[13-15] and statistical decay models[16] that provide interesting microscopic results and give predictions on possible MF mechanisms.

Within the Boltzmann-Uehling-Uhlenbeck (BUU) model it was shown that at the energy range 60–75 MeV/*A* “bubble” or “doughnut” structures can be formed depending on the stiffness of the nuclear EOS[17,18]. Later the formation of “doughnut” structures was confirmed experimentally[19]. Unfortunately up to now there is no model describing in details the underlying physical mechanisms of the exotic shapes formation in the head-on HIC. There are different possible ways to look for the explanation. One is to continue with the computer simulations. In

Supported by National Natural Science Foundation of China (NSFC) projects (Nos.11025524 and 11161130520) and National Basic Research Program of China (2010CB832903) and Ministry of Education, Science Youth and Sports of Ukraine project (No. M/175-2012).

* Corresponding author. *E-mail address:* Konstantin.Cherevko@gmail.com, fszhang@bnu.edu.cn

Received date: 2013-06-27

that case one should bear in mind that we are still far from having models that are formally well founded, practically applicable, and sufficiently realistic to be quantitatively useful[20]. Another way is to consider the qualitative Van der Waals and nucleon-nucleon interactions similarity[21] and to look for the explanation in thermodynamics[22-23] or hydrodynamics well developed for ordinary liquids. In that case a number of possible physical mechanisms being responsible for the phenomena can be suggested. Among them are the mechanism that includes the shockwave formation and interference and the one that studies the thermodynamic properties of the system (temperature, surface tension) together with the influence of the angular momentum on the system behavior[24]. The other possibilities are the possible capillary effects with "capons"[25] being formed on the nuclei surface and the spinodal decomposition of the system. Therefore, some deep analysis of the phenomena is needed to choose the appropriate decay channel.

The first step toward a better understanding of the process is the analysis of the qualitative picture that comes from the BUU calculations and the available experiments[17-19]. First to mention is the fact that the expanding velocity of the outer surface of the system is much smaller than the expanding velocity of the inner surface that suggests the importance of the surface effects. Second is the system behavior during the final stage. BUU calculations predict the simultaneous breakup with few fragments of similar masses and low kinetic energies. This suggests that the dynamic process might be responsible for the system evolution but at the breakup stage Coulomb force seems to be of great importance. Third is the angular distribution of fragments. In the case of soft EOS it is almost isotropic when for the stiff EOS fragments are in the plane perpendicular to the beam direction.

From all the above the hydrodynamic approach seems to be quite attractive as it allows explanation of the observed behavior of the system. In this work, we report an attempt to develop the hydrodynamic approach with the shockwave mechanism[17,26] that can explain the observed phenomena and reveal its physical nature.

2 Model description

When studying the system from the hydrodynamic point of view the question arises whether such a macroscopic theory works for the nuclear systems. Originally the idea to apply such a macroscopic theory to nuclei was introduced in 1970s–1980s by Siemens[27] and Stocker[28]. The domain of their studies was in a higher energy range than we are interested in, nevertheless, the existing confirmation for the applicability of hydrodynamics for nuclear systems suggests that it should be possible to use it for the energy range in focus[29].

The symmetry of the system allows the simplification of the model. Namely from the collision of two nuclei it is possible to change to the collision of a spherical nucleus of radius R with a rigid wall that moves toward it with the velocity v_0. The difference is in the viscous effects, therefore, the slip boundary condition on the wall surface should be added.

In our studies we start from the acoustic approximation developed in the theory of liquid droplet collisions[30,31]. Within this model according to Huygens principle the expanding nucleus edges emit wavelet that propagate with the sound velocity in all the directions and are the only source of the surface distortion. In that case the compression stage when the nucleus remains spherical lasts until the contact point velocity $v_c = v_0(R - v_0 t) / \sqrt{2Rv_0 t - v_0^2 t^2}$ [32] (can be found from the geometry of the system) is higher than the sound velocity v_s inside the nucleus (Fig.1). That first compression stage is characterized by the uniform pressure along z-axis and the pressure near the contact edge being higher than the pressure in the central part[31]. After that lateral jetting occurs and the pressure gradually decreases while the form of the nuclei is changing (Fig.1(a)).

In all the calculations a simple approximate relation between the sound velocity v_s and the particle velocity v_p is used:

$$v_s = v_{s0} + kv_p, \tag{1}$$

where k is a coefficient that is used as an adjusting parameter in the model and v_{s0} is the ambient sound velocity.

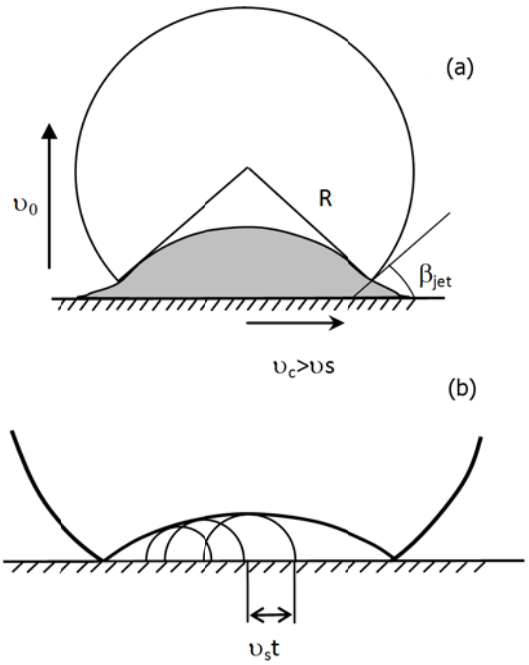

Fig.1 Initial stage of the drop collision with the rigid wall. (a) the picture of the system at $\tau>\tau_{jet}$.; compressed zone (according to the impact theory[32]) is shown in grey; (b) Huygens construction shows the shock envelope in the colliding system.

The compression part of the nuclear matter EOS[33]

$$U(\rho)=A\left(\frac{\rho}{\rho_0}\right)+B\left(\frac{\rho}{\rho_0}\right)^{\gamma}$$
$$P=\rho^2\frac{\partial E_B}{\partial\rho},\quad E_B=\frac{3}{5}E_F+\frac{1}{\rho}\int U(\rho)d\rho \tag{2}$$

together with the continuity equations and momentum and energy conservation

$$\frac{\partial\rho}{\partial t}+div(\rho\vec{\upsilon})=0$$
$$\frac{\partial(\rho\upsilon_i)}{\partial t}=-\frac{\partial(\rho\upsilon_i\upsilon_k+p\delta_{ik})}{\partial x_k} \tag{3}$$
$$\frac{\partial(\rho E)}{\partial t}+div(\upsilon(E+p))=0$$

are used for phenomena analysis. Parameters A, B and γ are chosen to give the different values of incompressibility[34,35]. $U(\rho)$, E_B, ρ, P and υ are the Skyrme type mean field potential, binding energy per nucleon, density, pressure and particle velocity, respectively. In addition simple geometrical considerations are used to find the relations between the normal and tangential components of sound and particle velocities in the disturbed and undisturbed parts of the system[32].

The introduced acoustic model is applicable during the first stage of the collision until there is no lateral jetting[31,32]. This fact allows calculating the jetting time from the anomalous behavior of the contact edge velocity (Fig.2). One may see that U_c decreases from infinity to some final value and after that starts increasing. Such a picture seems to be unphysical and the minimum should indicate the boundaries of the model applicability and therefore it corresponds to the jetting time.

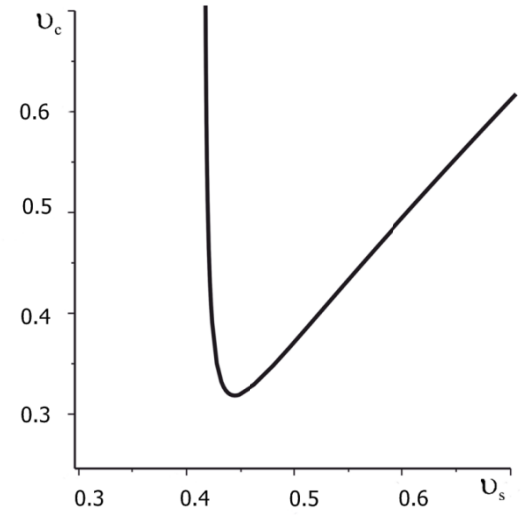

Fig.2 Contact edge velocity dependence on the sound velocity in the compressed part (normalized to the velocity of light).

When jetting occurs the shockwave starts to travel up along the free surface of the nucleus. This allows using the model of a jet formation between the rigid wall and the shockwave due to the pressure difference and the existing particles flow inside the nucleus. In this case assuming that the matter in the jet is at normal density ρ_0 it is possible to start with the hydrodynamic equations for the jet parameters[36] that take into account work against the surface forces L with the surface tension coefficient σ:

$$dL_s=8\pi\sigma RdR, \tag{4}$$

$$L=\frac{\pi}{2}R_{\text{jet}}^2\rho_{\text{bound}}\int_0^t\upsilon_{\text{jet}}^3dt. \tag{5}$$

From Eqs.(1)–(5) it is possible to calculate the main characteristics of the system geometry depending on the density at contact point ρ_{bound}:

$$R_{\rm jet}(t)=\frac{1}{32}\frac{\rho_{\rm bound}^2\upsilon_{\rm jet}^4t^2}{\rho_0\sigma}, \qquad (6)$$

where $R_{\rm jet}$ and $\upsilon_{\rm jet}$ are the size of the jet (Figs.3 and 4) and the particle velocity in the origin of the jet.

To check the hydrodynamic approach we have chosen ^{93}Nb+^{93}Nb system with the impact velocity V=0.34c that is the same as in the existing BUU calculations[17]. The parameter k=0.77 is adjusted from the comparison of jetting time in nuclear fluid dynamics calculations for ^{80}Kr+^{80}Kr at 400 MeV/A [26] and in our model.

3 Results and discussion

All the calculations are provided for the two types of the EOS. The results are presented in Tables 1 and 2.

Table 1 Comparison of the main characteristics of the process in the suggested hydrodynamic model and BUU calculations[17]

	This work	BUU[17]
Jetting time, $\tau_{\rm jet}$, fm/c	3.5	
Shape at $\tau_{\rm jet}$, $\Delta D/D$	0.2	
Pressure release time, fm/c	63	40~80
Maximum density, ρ/ρ_0	~1.76	~1.5

Table 2 Geometry of the system in the cases of soft (K=200) and stiff (K=400) EOS

	Soft EOS	Stiff EOS
Shape change, $\Delta D/D$	0.5	0.4
Geometry, $(D+2L)/D$	1.1	1.7
Time from collision, fm/c	24	21

First thing to mention is the good correspondence of the pressure release time (time when the expansion shockwaves reach the center of the nuclei and therefore the density of the system drops down) obtained in our calculations with that in the BUU (Table 1). Our calculations have shown that from the hydrodynamic point of view cases of "soft" and "stiff" EOS differ not only quantitatively but different mechanisms are involved in the system evolution. The geometry of the system for the two cases at a moment of time when the shockwaves reach the top of the nuclei and its evolution are shown in Figs.3 and 4. From the comparison one may see difference in the qualitative pictures for different EOS.

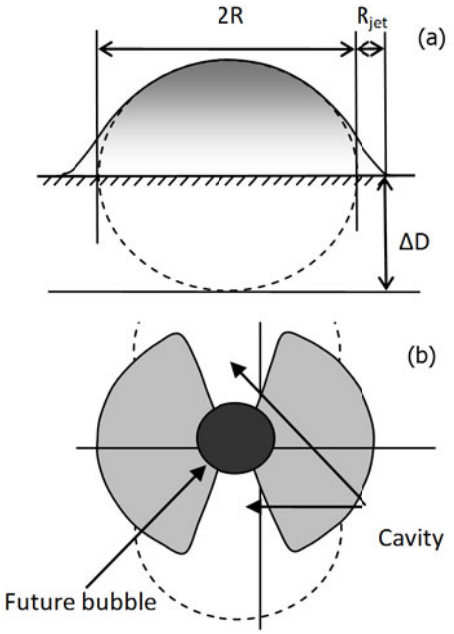

Fig.3 System geometry in the case of soft EOS. (a) time when the shockwaves reach the free surface of the nuclei; (b) cavity formation due to rarefaction. Future "bubble" is shown in black.

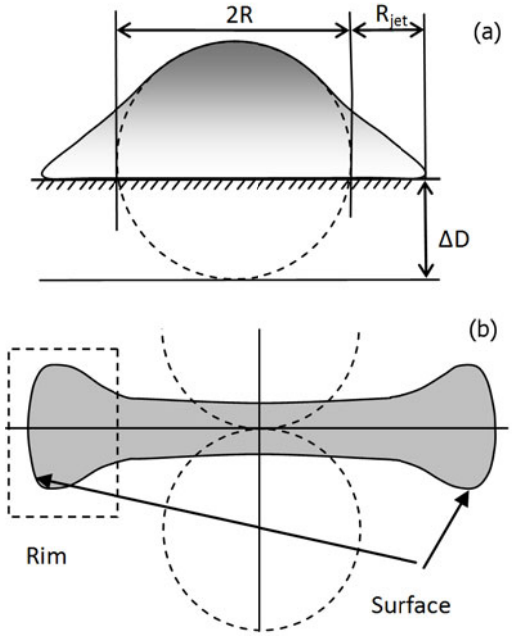

Fig.4 System geometry in the case of stiff EOS. (a) time when the shockwaves reach the free surface of the nuclei; (b) rim formation due to the surface and viscous forces. "Doughnut" structure is formed during the system evolution.

Soft EOS (Fig.3):

Such geometry allows the shockwaves produced on impact to be reflected from the free boundary and focused on the symmetry axis of the system. In that case rarefaction with cavity formation along the axis occurs (Fig.3(b)). Next steps in such a scenario are the

cavity collapse and bubble entrapment inside the system. This mechanism shows the possibility of the bubble formation in the collision.

Stiff EOS (Fig.4):

In that case system looks not like a spherical nuclei with small side parts (as it is for soft EOS) but rather like an expanding “pancake”. In our opinion this picture has some similarity with the problem of expanding liquid sheet[37]. Therefore we suggest that in this case the rarefaction along the symmetry axis does not play that important role but one rather observes the “pancake” becoming thinner and the thicker rim being formed due to the surface and viscous forces.

Both mechanisms give low values of the expanding velocities at the final state corresponding to the low kinetic energies of the fragments obtained in the BUU calculations.

We would also like to mention the possibility of the other geometry such as uniform system for different values of the impact energy or intermediate values of the incompressibility coefficient. Its occurrence as well defining the energy range where the exotic topologies can be observed require some further studies of the possible system splashing or recoil. Intuitively, the difference between the observed qualitative pictures has the origin in the initial stage when the compression pressure and temperature are different for different incompressibility coefficients. At this stage the only governing parameter is the sound velocity in the system. Viscous and surface forces come to play later on when the geometry has been defined already and govern the fragment formation processes.

Therefore, we suggest that the exotic structures formation in the head-on heavy ion collisions can be explained from the hydrodynamic point of view. In order to explain the breakdown of such structures and to predict the fragments mass distribution it is necessary to consider the possible Rayleigh-Plateau instabilities, capillary waves and the influence of the long range Coulomb forces at the final stage of the system evolution.

4 Conclusion

Suggested approach allows for a simple physical picture of the exotic structure formation in the head-on heavy ion collisions. The qualitative picture obtained within our model is in a good correspondence with the one observed within the BUU calculations and in the experiment. The straightforward link between the EOS and the exotic shapes of different topology is explained from the hydrodynamic point of view. Combination of the introduced hydrodynamic approach together with the microscopic calculations can reveal the physical nature of the multifragmentation phenomena and give the possibility to extract the data on the EOS from the head-on heavy ion collisions.

References

1 Bertch G F and Das Gupta S. Phys Rep, 1988, **160:** 189–233.

2 Abe Y, Ayik S, Reinhard P G, *et al.* Phys Rep, 1996, **275:** 49–196.

3 Baran V, Colonna M, Greco V, *et al.* Phys Rep, 2005, **410:** 335–466.

4 Li B A, Chen L W, Ko C M. Phys Rep, 2008, **464:** 113–281.

5 Baldo M and Maieron C. J Phys G: Nucl Part Phys, 2007, **34:** R243–R283.

6 Xie W J, Su J, Zhu L, *et al.* Phys Lett B, 2013, **718:** 1510–1514.

7 Kwiatkowski K, Fiedman W A, Woo L W, *et al.* Phys Rev C, 1994, **49:** 1516–1524.

8 Pan J and Gupta S. Phys Rev C, 1995, **51:** 1384–1392.

9 Zhang F S, Chen L W, Jin G M, *et al.* Phys Rev C, 1999, **60:** 064604.

10 Rodrigues M R D, Wada R, Hagel K, *et al.* J Phys: Conf Ser, 2011, **312:** 082009.

11 Hüfner J. Phys Rep, 1985, **125:** 129–185.

12 De Souza R, Le Neindre N, Pagano A, *et al.* Eur Phys J, 2006, **30:** 275–291.

13 Fuchs C and Wolter H H. Eur Phys J A, 2006, **30:** 5–21.

14 Zhang F S and Suraud E. Phys Lett B, 1993, **319:** 35–40.

15 Zhang F S and Suraud E. Phys Rev C, 1995, **51**: 3201–3210.

16 Tsang M B, Bougault R, Charity R, *et al.* Eur Phys J A, 2006, **30:** 129–139.

17 Bauer W, Bertsch G F, Schulz H. Phys Rev Lett, 1992, **69:** 1888–1891.

18 Xu H M, Gagliardi C A, Tribble R E, *et al.* Phys Rev C, 1993, **48:** 933–936.

19 Stone N T B, Bjarki O, Gualtieri E E, *et al.* Phys Rev Lett, 1997, **78:** 2084–2087.

20 Ono A and Randrup J. Eur Phys J A, 2006, **30:** 109–120.

21 Shlomo S, Kolomietz V M. Rep Prog Phys, 2005, **68:** 1–76.

22 Cherevko K V, Bulavin L A, Sysoev V M. Phys Rev C, 2011, **84:** 044603.

23 Su J and Zhang F S. Phys Rev C, 2013, **87:** 017602.

24 Wong C Y. Phys Rev Lett, 1984, **52:** 1393–1396.

25 Khodel V A. Sov J Nucl Phys, 1974, **19:** 404.

26 Stöcker H and Greiner W. Phys Rep, 1986, **137**:277–392.

27 Siemens P J and Rasmussen J O. Phys Rev Lett, 1979, **42:** 880–883.

28 Stocker H, Cusson R Y, Maruhn J A, *et al.* Z Phys A, 1980, **294:** 125–135.

29 Baumgardt H G, Schott J U, Sakamoto Y, *et al.* Z Phys A, 1975, **273:** 359–371.

30 Heynmann F J. J Appl Phys, 1969, **40:** 5113–5122.

31 Lesser M B. Proc R Soc Lond A, 1981, **377:** 289–308.

32 Haller K K, Poulikakos D, Venticos Y, *et al.* J Fluid Mech, 2003, **490:** 1–14.

33 Aichelin J. Phys Rep, 1991, **202:** 233–360.

34 Zhang F S. Z Phys A, 1996, **356:** 163–170.

35 Zhang F S and Ge L X. Nuclear multifragmentation. Beijing: Science Press, 1998.

36 Kutateladze S S and Styrikovich M A. Hydrodynamics of Gas-Liquid Systems, 1976, Moscow: Energy Publ.

37 Taylor G. Proc R Soc Lond A, 1959, **253:** 296–312.